J Mol Model (2005) 11: 503–508
DOI 10.1007/s00894-005-0259-4

ORIGINAL PAPER

Bella L. Grigorenko · Alexander V. Nemukhin
Raul E. Cachau · Igor A. Topol · Stanley K. Burt

Computational study of a transition state analog of phosphoryl transfer in the Ras–RasGAP complex: AlF_x versus MgF_3^-

Received: 6 January 2005 / Accepted: 17 January 2005 / Published online: 29 July 2005

Abstract The structures of the complexes between Ras•GDP bound to RasGAP in the presence of three probable γ-phosphate analogs (AlF_3, AlF_4^- and MgF_3^-) for the transition state (TS) of the hydrolysis of guanosine triphosphate (GTP) by the Ras-RasGAP enzymes have been modeled by quantum mechanical—molecular mechanical (QM/MM) calculations. These simulations contribute to the dispute on the nature of the TS in the hydrolysis reaction, since medium resolution X-ray crystallography cannot discern among stereochemically similar isoelectronic species (e.g., AlF_3 or MgF_3^-). The optimized geometry for each structure has been found starting from experimental coordinates of one of them (PDBID: 1WQ1). Direct comparison of the experimental and computed geometry configurations in the immediate vicinity of the active site suggests that MgF_3^- is the most likely candidate for the phosphate analog in the experimental structure.

Keywords GTP hydrolysis · Transition state analog · QM/MM modeling

Introduction

Hydrolysis of guanosine triphosphate (GTP) by G-proteins, leading to guanosine diphosphate (GDP) and inorganic phosphate (Pi), constitutes one of the most important enzymatic reactions responsible for normal and tumorigenic cellular signal transduction [1, 2]. Regular circulation between the GTP-bound ("ON") and GDP-bound ("OFF") states of human Ras proteins, stimulated by GTPase activating proteins (GAPs), may be suppressed by cancer-causing mutations at certain positions. The mechanism of this reaction and the role of mutations remain a subject of active debate.

The X-ray structure (PDBID: 1WQ1) of the complex between human H-Ras ($p21^{ras}$) bound to GDP and GAP-334 ($p120^{GAP}$) in the presence of a substitute of the γ-phosphate PO_3^- solved at a resolution 2.5 Å (estimated coordinate error 0.34 Å) [3] is an important contribution to structural studies of the GTP hydrolysis. This moiety often serves as a source of initial atomic coordinates for modeling the enzymatic reactions for the Ras–GAP protein complex with trapped GTP [4–6] and it is therefore important to understand all details of the structure.

Alumino-fluorides (AlF_x) are considered good substitutes for the γ-phosphate in crystal structures of GDP bound to G-proteins, and the arrangement GDP•AlF_x•H_2O has been proposed to be a mimic for TS. The AlF_4^- or AlF_3 species are assumed to be present in those structures [3, 7, 8]. In the 1WQ1 structure, the authors interpreted a maximum of electron density in the position usually occupied by the γ-phosphate as a trigonal aluminum fluoride, AlF_3, rather than a tetragonal AlF_4^- [3]. However, as discussed recently [9], another substitute, MgF_3^-, may be a plausible candidate for the TS analog for GTP hydrolysis, since it is difficult to distinguish in medium resolution X-ray structures between two stereochemically similar isoelectronic species. A quartenary complex RhoA•GDP•MgF_3^-•RhoGAP has been solved more recently at a higher resolution 1.8 Å (PDBID: 1OW3). Proton-induced X-ray emission has been used to determine the presence of magnesium and not aluminum in this structure. In a related system, the presence of MgF_3^- rather than presumably a PO_3^{n-} species in the intermediate of a phosphoryl transfer reaction in the β-phosphoglucomutase complex [10] was also discussed [11, 12].

B. L. Grigorenko · A. V. Nemukhin (✉)
Department of Chemistry, M. V. Lomonosov Moscow State University, Moscow, 119992, Russian Federation
E-mail: nemukhin@ncifcrf.gov
Tel.: +7-95-9391096
Fax: +7-95-9390283

R. E. Cachau · I. A. Topol · S. K. Burt
Advanced Biomedical Computing Center, SAIC Frederick, National Cancer Institute at Frederick, P. O. Box B, Frederick, MD 21702-1201, USA

Since all Ras-like magnesium-containing complexes are crystallized in a small excess of Mg [11], one cannot exclude that MgF_3^- is contained in the 1WQ1 structure as well. To study such a possibility, we explore the power of the hybrid quantum mechanical—molecular mechanical (QM/MM) methodology [13–17] for direct calculations of equilibrium geometry configurations of active sites GDP•AlF_3•H_2O, GDP•AlF_4^-•H_2O, and GDP•MgF_3^-•H_2O in the Ras–RasGAP protein complex. In every case, the starting set of atomic coordinates was that from the 1WQ1 structure. The results of our calculations were compared to the arrangement of atoms in the 1WQ1 structure. Such an analysis suggests that MgF_3^- is the most likely candidate for the substitute of the γ-phosphate in 1WQ1.

Methodology

Simulations were carried out by using the hybrid QM/MM technique in which the entire molecular system is partitioned into two parts, specified by the researcher. In the QM subsystem, the energy and forces acting on the atoms are computed according to QM equations, while the atoms within the MM subsystem interact between themselves following the classical rules with the selected set of force field parameters. The simulations described in this work have been performed by using our QM/MM implementation [18–20] based on effective fragment potential theory [21]. The essential feature of this flexible effective fragment QM/MM technique is that the coupling of QM and MM subsystems is treated at the ab initio level, while all empirical parameters are contained entirely in the MM part. Each effective fragment comprising of a few MM atoms interacts with the QM part, and polarization of the electron density of the quantum subsystem due to effects of the MM part is taken into account. All parameters of the effective fragment potentials are obtained in preliminary ab initio calculations and are not subject to change from one application to another. The computer program created on the base of the GAMESS [22] (more specifically, PC GAMESS (Granovsky A URL http://lcc.chem.msu.ru/gran/gamess/index.html) quantum chemistry package and molecular modeling system TINKER (Ponder J URL http://dasher.wustl.edu/tinker) allows us to scan the portions of a composite QM/MM potential energy surface and locate stationary points on the surface.

The QM part included the phosphate groups of GTP (and substitutes of the γ-phosphate), the lytic water molecule, nucleotide-associated magnesium ion (Mg^{2+}) and fractions of the side chains of of Gln61 and protonated Arg789. In total, 43 atoms constituted the quantum subsystem. A large fraction of the protein complex Ras–GAP was taken into account as the MM part. More specifically, 1622 atoms from the protein complex within approximately 20 Å distance from the P_γ atom of GTP were included to the MM subsystem subdivided to 488 effective fragments. In particular, the important "finger loop" ($L1_c$) from GAP was considered explicitly. Most of the MM subsystem referred to the Ras protein.

The search of minimum energy points on the composite QM/MM potential energy surface was performed as unconstrained minimization of the coordinates of the atoms in the QM subsystem and the positions of the effective fragments in the MM subsystem. The positions of remote effective fragments far away from the reaction center were not optimized. Consideration of saddle points on the potential surface connecting minimum energy configurations required sequences of constrained minimizations for an assumed reaction coordinate.

Geometry optimizations were carried out using the Hartree–Fock approach in the QM part. The polarized "LANL2DZdp ECP" basis set (and the corresponding pseudopotential for phosphorus) (URL http://www.emsl.pnl.gov/forms/basisform.html) was used for all atoms except magnesium. For the latter, the standard 6-31G basis set was employed. In the MM part, the AMBER set [23] of force-field parameters was applied.

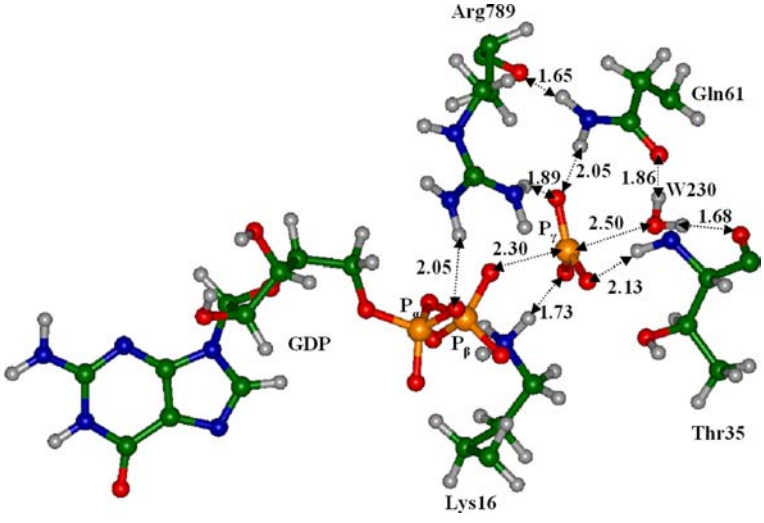

Fig. 1 Structure of the transition state as obtained by the QM/MM calculations. Shown are the key residues around the planar $P_\gamma O_3$ group. The distances, including those that involve hydrogen atoms, are given in Å

Results and discussion

In Fig. 1 we show the structure of the active site corresponding to the TS of the first stage of hydrolysis as computed by the QM/MM method. Descending from this point on the potential energy surface towards the entrance of the energy valley leads to the configuration of the reagents GTP + H_2O in an enzymatic environment. Descending from this point in the opposite direction leads to the reaction intermediate in which the P_γ–$O(P_\beta)$ bond in GTP is already broken, but the lytic water molecule is still in the pre-reactive state and the inorganic phosphate is not formed [6]. Proton transfers during a following stage of the reaction complete the hydrolysis process.

Selected distances between the atoms (including hydrogens) for the key residues and the water molecule around the γ-phosphate group are shown in Fig. 1 (the numbering of the residues is consistent with that of the 1WQ1 structure). Clearly, a united action of Arg789 of GAP, Gln61, Thr35 of Ras, and the lytic water molecule leads to a substantial spatial separation of the γ-phosphate of GTP from GDP. The water molecule (W230 according to the nomenclature of 1WQ1) is aligned by the carbonyl groups of Gln61 and Thr35. In turn, Arg789 keeps an important residue Gln61 fairly close to the active site. The planar $P_\gamma O_3$ group is included in the hydrogen bond network involving Gln61 and Thr35 as well as protonated Arg789 and Lys16.

Figures 2–4 shown the structures computed for the systems in which the γ-phosphate is replaced by AlF_3, AlF_4^- and MgF_3^-, respectively. While the structure shown in Fig. 1 corresponds to the saddle point on the potential energy surface (involving the true GTP species), the configurations shown in Figs. 2–4 refer to the minimum-energy points on their respective potential-energy surfaces. In every case, unconstrained optimization of variable geometry parameters was performed.

The left bottom panel in every Fig. 2, 3, or 4 refers to the same 1WQ1 experimental structure. The upper panels show superpositions of the configurations of the heavy atoms in 1WQ1 and of the corresponding model system containing AlF_3 (Fig. 2), AlF_4^- (Fig. 3) and MgF_3^- (Fig. 4). The right bottom panels in Figs. 2–4 show the same group of atoms (except a substitute in Figs. 3, 4) as in the left bottom panels. We note that the distances shown in the bottom panels of Figs. 2–4 refer only to the metal atom of a substitute but not to its ligands in order to avoid consideration of differences due to different numbers of fluorine atoms in the ligands.

The interpretation of results shown in Figs. 2–4 is straightforward. The model system containing MgF_3^- as a substitute of the γ-phosphate (Fig. 4) resembles the experimental structure 1WQ1 better than those with AlF_3 (Fig. 2) and AlF_4^- (Fig. 3). Comparison of the results obtained for the charged substitutes (AlF_4^- and MgF_3^-) and the uncharged one (AlF_3) to the experimental data leads to the conclusion that a negatively charged species is present in the crystal. The uncharged species (AlF_3) should be situated closer to the negatively charged β-phosphate (1.87 Å vs. 2.11 for AlF_4^-, or 2.24 for MgF_3^-, counting from $O(P_\beta)$) and further from the positively charged Arg789 (3.78 Å vs. 3.24 for AlF_4^-, or 3.49 for MgF_3^-, counting from nitrogen). Comparison of Figs. 3 and 4 show that of the two charged species, MgF_3^- corresponds better with the crystal data than AlF_4^-. It is worth noting that the equilibrium geometry configuration of the separated MgF_3^- species corresponds to a planar structure with Mg-F distances of 1.80 Å compared to that in the protein environment (Fig. 4) with the Mg-F distances 1.86, 1.87 and 1.89 Å.

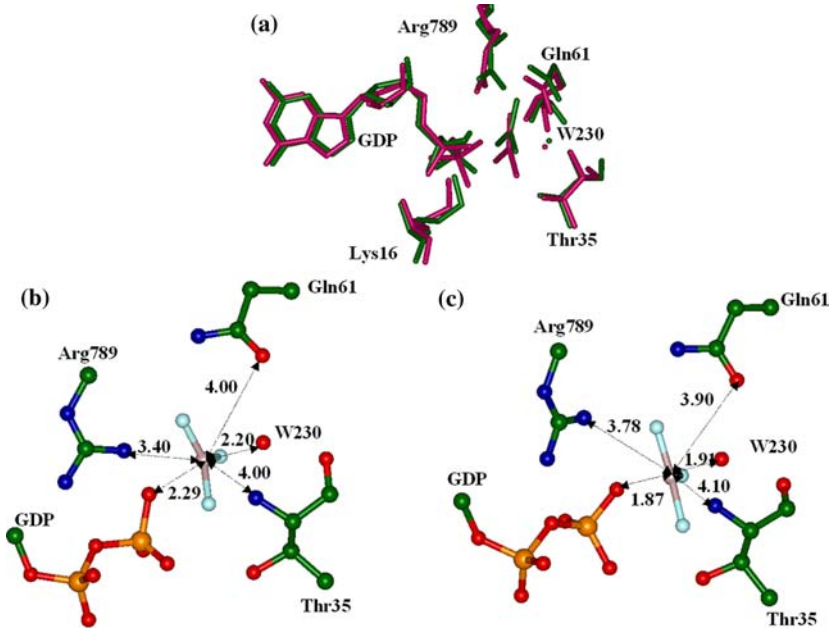

Fig. 2 Upper panel **(a)**—superposition of the crystal structure 1WQ1 (*green*) and the model structure containing the substitute AlF_3 (*wine*). Left bottom panel **(b)**—selected distances (Å) in the 1WQ1 structure; right bottom panel **(c)**—the corresponding distances in the model structure

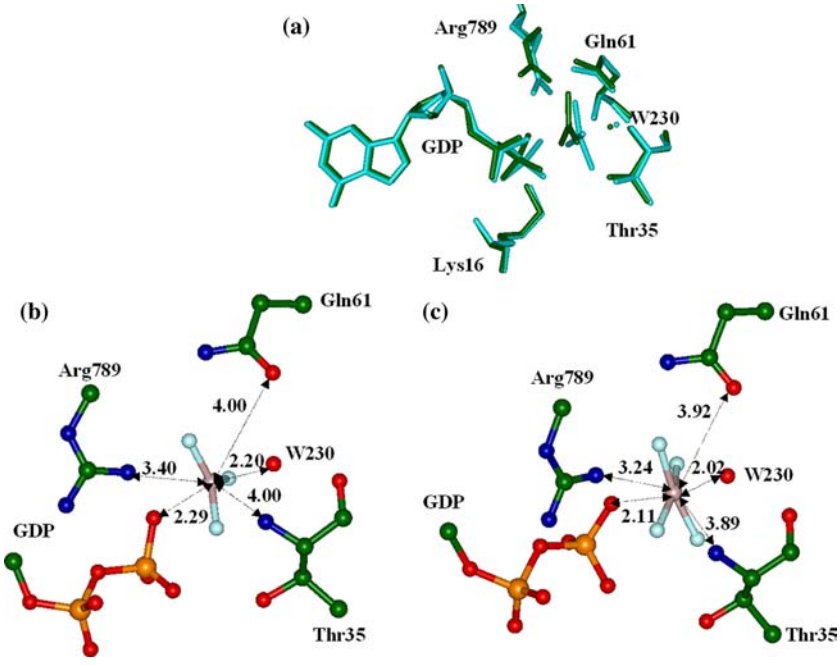

Fig. 3 Upper panel **(a)**—superposition of the crystal structure 1WQ1 (*green*) and the model structure containing the substitute AlF_4^- (*cyan*). Left bottom panel **(b)**—selected distances (Å) in the 1WQ1 structure; right bottom panel **(c)**—the corresponding distances in the model structure

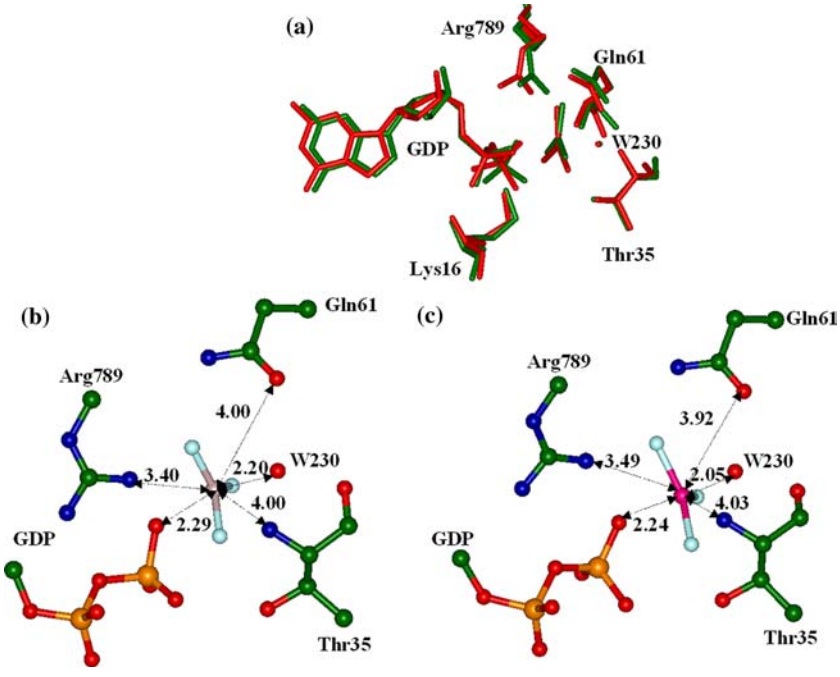

Fig. 4 Upper panel **(a)**—superposition of the crystal structure 1WQ1 (*green*) and the model structure containing the substitute MgF_3^- (*red*). Left bottom panel **(b)**—selected distances (Å) in the 1WQ1 structure; right bottom panel **(c)**—the corresponding distances in the model structure

It is instructive to add our simulation results to the data of Table 3 of Ref. [9] in which the authors summarized several interaction distances at the active site of the RhoA•GDP-RhoGAP complex with MgF_3^- (Fig. 5 of our paper was drawn following the motifs of Fig. 2c of Ref. [9]).

We include in Table 1 the data from Ref. [9], referring to the crystal structure of the RhoA•GDP–RhoGAP complex with MgF_3^- (second column), the data from the 1WQ1 structure, assuming the substitute as metal-trifluoride (column 3), and the data obtained in our simulations for the model system with MgF_3^-. Although considerable differences are noticeable in several places (first of all, for the positions of Arg of GAPs relative to GDP), the overall similarity is reasonable.

Conclusion

Direct comparison of the experimental and computed geometry configurations in the immediate vicinity of the active site shows that MgF_3^- is the most likely candidate

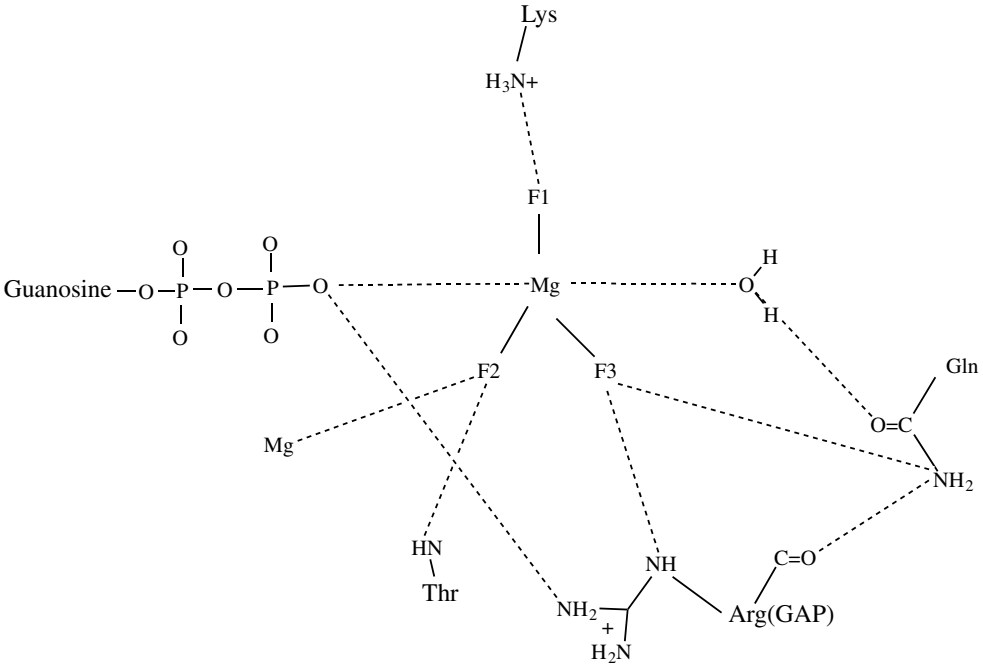

Fig. 5 Schematic diagram of the transition state analog under assumption that MgF_3^- stands as a substitute for the γ-phosphate (the same diagram as shown in Fig. 2c of Ref. [9])

Table 1 Selected distances at the active sites of the RhoA•GDP–RhoGAP complex with MgF_3^- [9]; of the Ras-RasGAP complex (1WQ1), assuming that it includes MgF_3^-; and of our model system with MgF_3^-

Interacting pairs	RhoA–RhoGAP, Ref. [9]	Ras–RasGAP (1WQ1)	Our model with MgF_3^-
Metal–lytic water	2.28	2.20	2.05
Metal–O(P_β)	2.02	2.29	2.24
Gln NE2–F3	2.92	2.93	2.63
Gln OE1–lytic water	2.58	2.93	2.81
Thr OG–nucleotide-associated Mg	2.22	1.97	2.27
F2–nucleotide-associated Mg	2.28	2.30	1.86
Thr main chain carbonyl–lytic water	2.88	3.03	2.63
Thr main chain NH–F2	2.93	2.99	3.04
GAP Arg main chain carbonyl–Gln NE2	2.90	2.67	2.76
GAP Arg NE–F3	2.89	4.25	4.42
GAP Arg NH2–O(P_β)	2.91	4.46	2.70
Lys NZ–F1	2.77	2.84	2.61

All distances are given in Å.

for the phosphate analog in the experimental structure of the complex between Ras•GDP bound to Ras–GAP in the presence of γ-phosphate substitute (PDBID: 1WQ1). The practical significance of these simulations is that the structure 1WQ1 provides an even better mimic of the transition state (TS) for GTP hydrolysis if a negatively charged species MgF_3^- represents a substitute for the γ-phosphate than the originally proposed composition with AlF_3.

Acknowledgements This work was supported in part by the grants from the Russian Foundation for Basic Research (04-03-32008). We thank the staff and administration of the Advanced Biomedical Computing Center for their support of this project. This project was funded in whole or in part with Federal funds from the National Cancer Institute, National Institutes of Health, under Contract No. NO1-CO-12400. The content of this publication does not necessarily reflect the views or policies of the Department of Health and Human Services, nor does mention of trade names, Commercial products, or organization imply endorsement by the U.S. Government.

References

1. Bourne HR, Sanders DA, McCormick F (1991) Nature 349:117–127
2. Sprang SR (1997) Ann Rev Biochem 66:639–678
3. Scheffzek K, Ahmadian MR, Kabsch W, Wiesmüller L, Lautwein A, Schmitz F, Wittinghofer A (1997) Science 277:333–338
4. Glennon TM, Villa J, Warshel A (2000) Biochemistry 39:9641–9651
5. Shurki A, Warshel A (2004) Proteins 55:1–10
6. Topol IA, Cachau RE, Nemukhin AV, Grigorenko BL, Burt SK (2004) Biochem Biophys Acta 1700:125–136
7. Bigay J, Deterre P, Pfister C, Chabre M (1985) FEBS Lett 191:181–185

8. Sondek J, Lambright DG, Noel JP, Hamm HE, Sigler PB (1994) Nature 372:276–279
9. Graham DL, Lowe PN, Grime GW, Marsh M, Rittinger K, Smerdon SJ, Gamblin SJ, Eccleston JF (2002) Chem Biol 9:375–381
10. Lahiri SD, Zhang G, Dunaway-Mariano D, Allen KN (2003) Science 299:2067–2071
11. Blackburn GM, Williams NH, Gamblin SJ, Smerdon SJ (2003) Science 301:1184c
12. Yarnell A (2003) Chem Eng News 81 37:30–31
13. Warshel A, Levitt M (1976) J Mol Biol 103:227–249
14. Singh UC, Kollman PA (1986) J Comp Chem 7:718–730
15. Field MJ, Bash PA, Karplus M (1990) J Comp Chem 11:700–733
16. Stanton RV, Hartsough DS, Merz KM (1995) J Comp Chem 16:113–128
17. Assfeld X, Rivail J-L (1996) Chem Phys Lett 263:100–106
18. Grigorenko BL, Nemukhin AV, Topol IA, Burt SK (2002) J Phys Chem A 106:10663–10672
19. Nemukhin AV, Grigorenko BL, Topol IA, Burt SK (2003) J Comp Chem 24:1410–1420
20. Nemukhin AV, Grigorenko BL, Rogov AV, Topol IA, Burt SK (2004) Theor Chem Acc 111:36–48
21. Gordon MS, Freitag MA, Bandyopadhyay P, Jensen JH, Kairys V, Stevens WJ (2001) J Phys Chem A 105:293–307
22. Schmidt MW, Baldridge KK, Boatz JA, Elbert ST, Gordon MS, Jensen JH, Koseki S, Matsunaga N, Nguyen KA, Su SJ, Windus TL, Dupuis M, Montgomery JA (1993) J Comp Chem 14:1347–1356
23. Cornell WD, Cieplak P, Bayly CI, Gould IR, Merz KM, Ferguson DM, Spellmeyer DC, Fox T, Caldwell JW, Kollman PA (1995) J Am Chem Soc 117:5179–5197